Pleiotropy enables specific and accurate signaling in the presence of ligand cross talk

Duncan Kirby[a], Jeremy Rothschild[a], Matthew Smart[a], and Anton Zilman[a,b*]
[a] *University of Toronto, 60 Saint George st, Toronto, ON M5S1A7, Canada and*
[b] *Institute for Biomaterials and Bioengineering, University of Toronto, 164 College St , Toronto, ON M5S 3G9, Canada*

Living cells sense their environment through the binding of extra-cellular molecular ligands to cell surface receptors. Puzzlingly, vast numbers of signaling pathways exhibit a high degree of cross talk between different signals whereby different ligands act through the same receptor or shared components downstream. It remains unclear how a cell can accurately process information from the environment in such cross-wired pathways. We show that a feature which commonly accompanies cross talk - signaling pleiotropy (the ability of a receptor to produce multiple outputs) - offers a solution to the cross talk problem. In a minimal model we show that a single pleiotropic receptor can simultaneously identify and accurately sense the concentrations of arbitrary unknown ligands present individually or in a mixture. We calculate the fundamental limits of the signaling specificity and accuracy of such signaling schemes. The model serves as an elementary "building block" towards understanding more complex cross-wired receptor-ligand signaling networks.

arXiv:1911.05895v4 [q-bio.MN] 2 Apr 2021

I. INTRODUCTION

Receptor signaling via soluble ligand molecules enables living cells to communicate with each other and with their environment, and is the main mode of multicellular coordination in the immune, nervous, endocrine and other systems, as well as in complex populations of microorganisms. In a typical signaling pathway, binding of a ligand to a cell surface receptor activates a cascade of intracellular events that eventually lead to responses such as cellular differentiation [1–4], phenotypic change [4–7], or a change in cellular motility [8–12]. For reliable and precise communication, receptor signaling often needs to be specific, accurate, rapid and robust to molecular noise and cellular heterogeneity [13–20]. However, fundamental physical constraints often place these different signaling goals at odds with each other [17, 18, 21–24], and different signaling pathways have evolved to optimize different aspects of information transmission such as molecular specificity [18, 22, 25], sensitivity [5, 18, 26], accuracy of concentration sensing [9, 28–30], and speed [24, 31–33].

Puzzlingly, receptor signaling pathways frequently exhibit a high degree of cross talk whereby multiple ligands act through shared cell surface receptors or downstream signaling components [34–45]. Another puzzling feature that commonly accompanies cross talk is receptor pleiotropy - the ability of a receptor to produce more than one type of output. This combination of features commonly results in "hourglass" shaped input-output networks [41, 42, 46–49]. This challenges the classical "one ligand/one signal" paradigm [4], while raising the question of how signaling pathways are able to effectively transmit information under such conditions [22, 30, 42, 50–55].

Ligand-receptor cross talk poses a fundamental problem for effective signal transmission which can be illustrated through an example of the conflict between two goals: 1) identification of the ligand out of many others that bind the same receptors in order to produce a specific response (which we denote as "specificity") and 2) quantification of the amount of the ligand in order to accurately respond to different concentrations (which we denote as "accuracy"). In a classical view of ligand-receptor binding, the signaling response is dictated by the average receptor occupancy $P = (c/K_d)/(1 + c/K_d)$, where c is the ligand concentration and K_d is the equilibrium dissociation constant of the ligand-receptor binding [56]. The ligand concentration and the dissociation constant enter into this expression only through their ratio, c/K_d, and identical receptor occupancies can be realized by a weakly binding ligand present at a high concentration, or a strongly binding one at a low concentration. Hence, based on the receptor occupancy alone, it is generally impossible to unambiguously determine which ligand is bound to the receptor while also accurately quantifying its concentration (see 1. This example is a manifestation of a more general inference problem that arises in the presence of cross talk: the difficulty of unambiguously inferring multiple input variables - in this case the ligand concentration ("quantity") and its identity measured as receptor binding affinity ("quality") - from one output variable (in this case receptor occupancy). This problem is exacerbated when multiple ligands that bind the same receptor are present simultaneously in a mixture, as the number of unknown ligand identities and concentrations increases. It remains unclear how the cell can unambiguously determine the composition and the concentrations of the ligands in the mixture.

Several recent works addressed some aspects of this problem. In particular, [30, 42, 51–53] focused on the effects of cross talk on the accuracy of sensing the concentration of a cognate ligand in the presence of non-specific ligands. Such problems commonly arise in the context of cellular chemotaxis driven by concentration gradients of food or chemoattractants. Using an extension of the classical Berg-Purcell framework [13–15, 27, 57], it was

* zilmana@physics.utoronto.ca

shown that, given sufficient separation between the affinities of the specific and non-specific ligands, detection and accurate sensing of the concentration of the high-affinity ligand is possible even if it is outnumbered by the low-affinity ligand [30, 52]. Furthermore, under certain conditions the cell is able to determine the concentration of the non-specific ligands as well [52]. In further work, it was also shown that the accuracy can in some cases be increased by a more complicated ligand-receptor network that includes two cross-wired receptors [51]. The results of these works largely rely on several important assumptions: 1) only two ligand types (specific and non-specific) can bind the same receptor, 2) identity of the cognate ligand, as expressed via its binding affinity to the receptor, is known and 3) the inference of the ligand concentration is based on the whole sequence of ligand-receptor binding and unbinding times.

In a related set of problems, inspired by T cell receptor (TCR) signaling, the cell needs to efficiently filter out the weak affinity "self" (non-specific) ligands but to sensitively respond to even very low concentrations of the strong affinity "non-self" (specific) ligand. One proposed solution, relying on the "adaptive sorting" modification of the classical kinetic proofreading (KPR) scheme, enables "absolute discrimination" between different ligands based on their affinities, unconfounded by their concentrations [18, 23]. Kinetically different, but conceptually similar mechanisms are involved in the absolute ligand discrimination by dimeric receptors [22]. In a different approach to the same problem, [17, 30] studied the probability of detection of a cognate ligand present at a low concentration over a background of "wrong" ligands. However, these works focused on the sensitive detection of the ligand presence rather than on the identification of different ligands.

In this paper we consider a general problem of specific (ligand identification) and accurate (concentration measurement) sensing in the presence of cross talk in signaling pathways with multiple ligands acting through a single shared receptor. This problem is motivated by the observation that in many signaling systems cells are capable of providing substantially different responses to multiple different ligands acting through the same pathway (specificity/identification) while maintaining dose response sensitivity for each of them (accuracy/quantification), even if the ligands are present in complex mixtures. This scenario appears in a number of signaling pathways such as cytokine and chemokine signaling, some aspects of T cell response, G-protein coupled receptor (GPCR) signaling and others[41, 55, 58, 59]. The ability to specifically and accurately respond to different cytokine combinations is necessary for cells to respond to different physiological situations which are encoded by different combinations of signaling molecules [38, 60, 61]. This raises the question of how cells are able to sense mixed signals both specifically and accurately in the presence of cross talk [41, 42].

We show that signaling pleiotropy - the ability of the receptor to produce several different signals in response to ligand binding - provides a solution to the specificity-accuracy problem both when the ligands are present alone or in mixtures. We introduce a minimal, biologically motivated model of a pleiotropic receptor capable of binding a large number of ligands, and show that it can unambiguously determine both the receptor binding affinities and the concentrations of an arbitrary number of ligands. Furthermore, we calculate the fundamental limits on the specificity and accuracy of such sensing in the presence of noise both at the receptor level and downstream.

We further show that signaling pleiotropy enables specific and accurate sensing of the affinities and concentrations when two ligands are present in a mixture, demonstrating that the receptor signaling scheme discussed here can serve as a "building block" for the general problem of signaling cross talk in mixtures of multiple ligands.

The paper is structured as follows. In section II A we define the mathematical framework, formulate the problem of the specificity-accuracy trade-off for a non-pleiotropic receptor and introduce the mathematical definitions of specificity and accuracy. In section II B we introduce the pleiotropic receptor, show that it resolves the specificity-accuracy problem, and calculate the fundamental limits on the sensing specificity and accuracy. In section II C we show how our model resolves the cross talk problem in more complex cases where multiple ligands are present simultaneously. We conclude with a discussion and possible generalizations in section III.

II. RESULTS

A. Non-pleiotropic receptor

The accuracy of concentration sensing by a molecularly specific receptor that binds a ligand of one type has been investigated in a large number of works [15, 27, 30, 52, 62, 63], starting with the pioneering work of Berg and Purcell [13]. In this section, we extend the framework developed in these works to address the problem of specificity - the ability of the receptor to distinguish between different molecularly distinct ligands.

To investigate the general problem of signaling specificity and accuracy, in this section we introduce a signaling receptor capable of binding a large number of ligands, as illustrated in Fig. 1. Here we confine ourselves to the situation where the receptor is exposed to a single ligand, out of many possible ones that bind the same receptor due to ligand cross talk, at concentration c (see section II C for generalization to ligand mixtures).

The identity of a ligand is defined by its binding and unbinding rates to the receptor, $k_{\rm on}$ and $k_{\rm off}$, respectively. In general, these rates depend in a non-trivial fashion on the molecular details of the receptor-ligand interface [37, 41, 45] and its surroundings [15, 64, 65]; for simple monomolecular binding they combine into the equilib-

rium dissociation constant $K_d \equiv k_{\rm off}/k_{\rm on} \propto e^{-\epsilon}$ where ϵ is the ligand-receptor binding energy [66]. For simplicity, we assume that the binding rate constant $k_{\rm on}$ is independent of the ligand identity, which is then fully captured by its unbinding rate $k_{\rm off}$ (or, alternatively, the dissociation constant $K_d = k_{\rm off}/k_{\rm on}$.

While bound by a ligand, a non-pleiotropic receptor produces a single type of downstream signaling molecule at a rate k_p, which serves as the readout of the ligand presence outside the cell. This signaling mechanism is common to a large number of pathways, e.g. where the active form of the output molecule is produced via phosphorylation by a receptor-bound kinase [4, 67]. Functionally, this output variable essentially measures the bound time of the receptor [15]. The results which follow are trivially extended to N independent copies of the receptor, as explained below.

The state of the system at time t is described by the probability $P_i^n(t)$ to be in the occupancy state i ($i = 1$ when the receptor is occupied by the ligand, 0 otherwise) and have produced n output molecules by time t. The ensemble dynamics of the system are described by the master equation for the probability $P_i^n(t)$ [68–70]:

$$\begin{aligned}\frac{d}{dt}P_0^n &= k_{\rm off}P_1^n - k_{\rm on}cP_0^n \\ \frac{d}{dt}P_1^n &= k_{\rm on}cP_0^n - k_{\rm off}P_1^n + k_pP_1^{n-1} - k_pP_1^n\end{aligned} \tag{1}$$

At receptor occupancy steady state, the probability of the receptor being occupied is $p = x/(1+x)$ where $x = c/K_d$. For simplicity and connection to previous work [27, 30], we currently neglect degradation of the output molecules.

The master equation (1) can be solved using the generating function $G_i(s,t) = \sum_n s^n P_i^n(t)$. The dynamics of the vector $\mathbf{G} = (G_0(s,t), G_1(s,t))$ are then described by the equation [68, 70]:

$$\begin{aligned}&\frac{d}{dt}\mathbf{G}(s,t) = \hat{\mathbf{M}}\mathbf{G}(s,t) \\ &\text{with } \hat{\mathbf{M}} = \begin{bmatrix} -k_{\rm on}c & k_{\rm off} \\ k_{\rm on}c & -k_{\rm off} + k_p(s-1)\end{bmatrix},\end{aligned} \tag{2}$$

yielding the general solution at time t as $\mathbf{G}(s,t) = e^{\hat{\mathbf{M}}t}\mathbf{G}(s,0)$. Assuming that the receptor is at steady state at the beginning of the measurement (defined as $n = 0$), the initial condition is $\mathbf{P}^0 = (1-p, p)$ for $n = 0$ and $\mathbf{P}^n = (0,0)$ otherwise, and therefore $\mathbf{G}(1,0) = (1-p,p)$. Similar results can be obtained if the receptor is initially unoccupied with $\mathbf{G}(1,0) = (1,0)$ producing identical results in the limit of large numbers of binding events, $k_{\rm off}t \gg 1$ which is the focus of this paper (see Supplemental Material [71] for details).

The mean and the variance of n are calculated as $\langle n\rangle = \sum_i \frac{\partial G_i(s,t)}{\partial s}|_{s=1}$ and $\langle \delta n^2\rangle = \sum_i \frac{\partial G_i(s,t)}{\partial s^2}|_{s=1} + \langle n\rangle - \langle n\rangle^2$. For $k_{\rm off}t \gg 1$, these are

$$\begin{aligned}\langle n\rangle &= k_p t\frac{x}{1+x} \\ \langle \delta n^2\rangle &= k_p t\frac{x}{1+x} + \frac{2k_p^2 t}{k_{\rm off}}\frac{x}{(1+x)^3}.\end{aligned} \tag{3}$$

In the long-time limit, defined as $\min(k_{\rm off}, k_p) \gg 1/t$, the probability distribution of n, $P(n|c, k_{\rm off})$, tends to a Normal distribution $\mathcal{N}(\langle n\rangle, \langle \delta n^2\rangle)$, $P(n|c,k_{\rm off}) = (2\pi\langle\delta n^2\rangle)^{-1/2}\exp(-(n-\langle n\rangle)^2/(2\langle\delta n^2\rangle))$ (see Supplemental Material [71]). Physically, these results reflect the fact that the receptor produces molecules at rate k_p while it is occupied (on average $x/(1+x)$ fraction of the time t). For the variance, the first term reflects fluctuations in the readout n for fixed bound time, and the second term reflects fluctuations in the bound time; see also Supplementary Material Section D. Note that the variance of n scales as $k_p t$, in accordance with the Central Limit Theorem.

Specificity and accuracy of the non-pleiotropic receptor. The classical problem of accuracy can be stated as the estimation of the concentration c from the number of signaling molecules n when $k_{\rm off}$ is known - a situation realized when the receptor is highly molecularly specific and can bind only one ligand type [13, 15]. We formulate the problem of specificity in a similar manner - as the estimation of $k_{\rm off}$ given n. Note that this specificity definition is different from the common measure of specificity as the ratio of the mean number of sensing molecules produced by different ligands. However, it is impossible to unambiguously estimate both c and $k_{\rm off}$ from a single measurement of the output variable n - illustrating the fundamental specificity-accuracy trade-off - because the same number of output molecules can be produced by a weaker ligand at higher concentration as by a stronger ligand at lower concentration. This point is illustrated in Fig. 1(b). Within this scheme, only the combination $x = k_{\rm on}c/k_{\rm off}$ can be inferred from n.

One useful framework to interrogate these ideas is statistical inference theory [72]. Here we provide approximate but intuitive derivations; exact numerical derivations are provided in the Supplemental Material [71]. To help illustrate the specificity-accuracy trade-off, we first focus on the determination of the ligand identity through the estimation of $k_{\rm off}$. Assuming the concentration c is known, an intuitive estimate of $k_{\rm off}$ given n, $k_{\rm off}^*(n)$, is provided via maximization of the likelihood $P(n|k_{\rm off})$ (or equivalently, the log-likelihood $L = \ln P$) over $k_{\rm off}$; this procedure is known as maximum likelihood estimation (MLE) [27, 62]. This is equivalent to the maximization of the posterior probability $P(k_{\rm off}|n) = P(n|k_{\rm off})P(k_{\rm off})/\int P(n|k_{\rm off})P(k_{\rm off})dk_{\rm off}$ for a uniform prior $P(k_{\rm off})$ [62]. In the long time limit, the likelihood $P(n|k_{\rm off})$ is well-approximated by a Normal distribution, peaked around $\langle n\rangle$. Neglecting the logarithmic terms in $L(n|k_{\rm off})$, the MLE $k_{\rm off}^*$ is given by the

condition $\langle n \rangle (k^*_{\rm off}) = n$ [15, 72], yielding

$$\frac{k^*_{\rm off}}{k_{\rm on} c} = \frac{k_p t}{n} - 1 \tag{4}$$

For a given n, expanding the likelihood about $k^*_{\rm off}(n)$ gives, to lowest order, a Normal distribution whose variance $\delta k^2_{\rm off} = -\left(\frac{\partial^2 \ln P(n|k_{\rm off})}{\partial k^2_{\rm off}}|_{k^*_{\rm off}}\right)^{-1}$ is a measure of the uncertainty in the estimate $k^*_{\rm off}$ [62]. Repeating this over the distribution $P(n|k_{\rm off})$ of possible outcomes n gives the average uncertainty $\langle \delta k^2_{\rm off} \rangle = -\left\langle \frac{\partial^2 \ln P(n|k_{\rm off})}{\partial k^2_{\rm off}} \right\rangle^{-1}$; the quantity $\left\langle -\frac{\partial^2 \ln P(n|k_{\rm off})}{\partial k^2_{\rm off}} \right\rangle$ is known as the Fisher Information [72]. In the saddle point approximation, accurate for sharply peaked likelihoods, this simplifies to $\langle \delta k^2_{\rm off} \rangle \simeq -\left(\frac{\partial^2 \ln P(n|k_{\rm off})|_{k_{\rm off}=k^*_{\rm off}}}{\partial k^2_{\rm off}}\right)^{-1} \simeq \langle \delta n^2 \rangle / (\partial \langle n \rangle / \partial k_{\rm off})^2$ [15, 62, 72] (see Supplemental Material [71]). This expression has a simple intuitive meaning: fluctuations in n resulting from the stochasticity of binding-unbinding and production events lead to uncertainty in the estimate $k^*_{\rm off}$, as illustrated in Fig. 1(c). Importantly, although heuristically derived here on the basis of the ML estimate, the Fisher Information formalism applies more generally as a lower bound on the estimate error [72].

Using the non-dimensionalized quantity $x = k_{\rm on} c / k_{\rm off}$, the relative average error (squared) of the estimate becomes

$$\frac{\langle \delta k^2_{\rm off} \rangle}{k^2_{\rm off}} = \frac{\langle \delta x^2 \rangle}{x^2} = \frac{1}{k_p t} \frac{1+x}{x} \left((1+x)^2 + 2 \frac{k_p}{k_{\rm off}} \right). \tag{5}$$

For N independent copies of the receptor on the cell surface, the above expression is multiplied by N^{-1} [14].

These results are summarized in Figs. 1(d) and 1(e), which show the squared relative error of the estimate x (equivalently, $k_{\rm off}$), scaled by $k_p t/N$, as a function of dimensionless quantities $k_{\rm on} c/k_p$ and $k_{\rm off}/k_p$. We scale the squared relative error by $k_p t/N$ to present the time-independent part of the cell's estimation error. The blue region in Fig. 1(d) indicates where the error in the estimate (i.e. $\sqrt{\langle \delta x^2 \rangle / N}$) is less than 33% the true value, which we have chosen as a cutoff for "good" estimation performance. This cutoff is chosen somewhat arbitrarily, as the cell can improve its estimation accuracy by increasing the number of copies N of the receptor or by increasing the signal integration time t. To provide a conservative estimate, we visualize these results with $N = 10^2$, which is at the lower end of the biological range of receptor expression levels [73].

As expected, the typical error of the estimate of $k_{\rm off}$ diverges both for $x \to 0$ and $x \to \infty$ because at very fast unbinding rates the receptor does not produce enough signaling molecules for a meaningful statistical estimate, while at very slow unbinding rates the receptor occupancy saturates independent of either affinity or concentration. The value of x at which the optimal specificity is achieved increases with the concentration c and saturates to $x = 1/2$ for $c \gg 1$.

The problem of concentration sensing accuracy can be similarly formulated as the problem of estimating c from n at fixed $k_{\rm off}$ via maximization of the likelihood $P(n|c)$ over c [27]. Following the same approach as in Eqs. (4) and (5), the best estimate and its variance are again given by $\frac{k_{\rm on} c^*}{k_{\rm off}} = \frac{n}{k_p t} \frac{1}{1 - n/k_p t}$ and $\frac{\langle \delta c^2 \rangle}{c^2} = \frac{\langle \delta x^2 \rangle}{x^2} = \frac{\langle \delta k^2_{\rm off} \rangle}{k^2_{\rm off}}$.

Interestingly, the ML estimate of the concentration based on n is mathematically identical to that of Endres and Wingreen [27], which was based on a more informative likelihood function containing the whole series of binding and unbinding events. We return to this point in the Discussion.

In the limit $k_p \gg k_{\rm off}$ the expression for the concentration sensing accuracy reduces to the classical Berg-Purcell expression $2(1+x)/(k_{\rm on} c t) = 1/(2Dac(1-p)t)$ where $4Da = k_{\rm on}$ [13, 15], as each binding event in this regime produces multiple signaling molecules, and the sensing accuracy is limited by the fluctuations in receptor occupancy considered in [13]. Notably, for finite $k_p/k_{\rm off}$, fluctuations in the production of the output molecule n play an important role, as they cause the divergence of the estimate accuracy observed at high x in Eq. 5 - a feature absent from the models that consider only the noise in the receptor occupancy [13, 27]. In particular, the concentration at which the best estimate is obtained changes significantly with $k_p/k_{\rm off}$, and is not necessarily close to $x = 1$, the point of highest response sensitivity to concentration changes.

However, crucially for the main question of this paper, it is impossible to estimate both c and $k_{\rm off}$ simultaneously because the distribution $P(n|c, k_{\rm off})$ does not possess a well defined peak in the $(c, k_{\rm off})$ space but rather a ridge along the line $\frac{c}{K_d} = \frac{n}{k_p t} \frac{1}{1 - n/k_p t}$, as shown in Fig. 1(f). This could in principle be resolved by careful selection of a prior on $(c, k_{\rm off})$, which in practice implies additional assumptions regarding the molecular inference machinery, and lies outside the scope of the present work.

B. Pleiotropic receptor

In contrast to the results of the previous section, it is possible to unambiguously estimate both $k_{\rm off}$ and c simultaneously if the receptor is pleiotropic (i.e. produces more than one output signal upon ligand binding). In this section, we extend the model of the previous section to include a second sensing molecule, inspired by G-protein coupled receptor (GPCR) signaling [58, 74], shown in Fig. 2(a). In this scheme, the G-protein (GP)-like molecule is pre-bound to the intracellular domain of the receptor and detaches once a ligand binds. For simplicity, we assume that upon ligand unbinding the receptor quickly rebinds a new GP-like molecule and is ready for signaling. Although, as defined, this type of sensing molecule has an unnatural fea-

ture that it can be produced even for infinitesimally short binding events [51], the model is sufficient to demonstrate the role of pleiotropy in ligand sensing. Biologically, combined kinase-phosphorylation and G-protein signaling has been reported in some cytokine receptors [36] and other immune receptors [75].

We denote the total number of GP-like molecules produced by time t as m, which effectively serves as a count of the number of binding events rather than the total binding time (which is measured by n, as defined in the previous section) [27, 30, 52]. As shown below, this model naturally allows joint determination of the ligand identity and its quantity $(c, k_{\rm off})$ from the two signaling outputs (n, m) (see Fig. 2).

The system is now described by the probability of being in a given state at time t, $P_i^{n,m}(t)$, where i denotes the receptor state ($i = 1$ if bound by a ligand, 0 if unbound) and n and m are the numbers of the sensing molecules accumulated by time t. Similar to the previous section, the dynamics of the system are described by the following master equation:

$$\begin{aligned}\frac{d}{dt}P_0^{n,m} &= k_{\rm off}P_1^{n,m} - k_{\rm on}cP_0^{n,m}\\ \frac{d}{dt}P_1^{n,m} &= k_{\rm on}cP_0^{n,m-1} - k_{\rm off}P_1^{n,m} + k_pP_1^{n-1,m} - k_pP_1^{n,m}.\end{aligned} \tag{6}$$

This master equation can be solved using the generating function technique, similar to Eq. (2) in the previous section (see details in the Supplemental Material [71]). The mean and the variance of n remain the same as in Eq. (3). The mean of m, its variance $\langle\delta m^2\rangle$ and the covariance $\langle\delta n\delta m\rangle$ are, in the $k_{\rm off}t \gg 1$ limit,

$$\begin{aligned}\langle m\rangle &= k_{\rm off}t\frac{x}{1+x}\\ \langle\delta m^2\rangle &= k_{\rm off}tx\frac{1+x^2}{(1+x)^3}\\ \langle\delta n\delta m\rangle &= k_ptx\frac{1-x}{(1+x)^3}.\end{aligned} \tag{7}$$

These results can also be derived using renewal process theory (see Supplemental Material [71]). Note that at small x, n and m are correlated because in the low concentration/weak binding limit the overall bound time is proportional to the number of events. By contrast, at large x, n and m are anti-correlated because in this regime a time series with more binding-unbinding events results in lower overall bound time. However, for $x \to \infty$, $\langle\delta n\delta m\rangle \to 0$ because the receptor is occupied all the time, and the number of binding events is not correlated with the total bound time.

Specificity and accuracy of the pleiotropic receptor. The crucial feature of Eq. (7) is that the variable m depends differently on the unbinding rate $k_{\rm off}$ and the concentration c compared to the variable n of Eq. (3), which allows the estimation of both c and $k_{\rm off}$. As before, we assume that k_p and $k_{\rm on}$ are fixed constants, hardwired into the molecular machinery of the cell. In the long time limit, the likelihood $P(n, m|c, k_{\rm off}) \equiv P_0^{n,m} + P_1^{n,m}$ is well approximated by a multivariate Normal distribution $\mathcal{N}(\boldsymbol{\mu}, \hat{\mathbf{C}})$ with mean and covariance

$$\boldsymbol{\mu} = \begin{bmatrix}\langle n\rangle\\ \langle m\rangle\end{bmatrix} \quad \text{and} \quad \hat{\mathbf{C}} = \begin{bmatrix}\langle\delta n^2\rangle & \langle\delta n\delta m\rangle\\ \langle\delta m\delta n\rangle & \langle\delta m^2\rangle\end{bmatrix}, \tag{8}$$

so that

$$P(n, m|c, k_{\rm off}) = (Z)^{-1}\exp\left(-\frac{1}{2}(\mathbf{n}-\boldsymbol{\mu})^T\hat{\mathbf{C}}^{-1}(\mathbf{n}-\boldsymbol{\mu})\right),$$

where $\mathbf{n} = (n, m)$ and normalization factor $Z = (2\pi)^2\det(\hat{\mathbf{C}})^{1/2}$.

Estimates for $k_{\rm off}$ and c can be found in the same manner as in the previous section, by maximizing the likelihood $P(n, m|c, k_{\rm off})$ over c and $k_{\rm off}$, which yields:

$$c^* = \frac{k^*_{\rm off}}{k_{\rm on}}\frac{n/(k_pt)}{1-n/k_pt} \quad k^*_{\rm off} = k_p\frac{m}{n}. \tag{9}$$

Interestingly, the same ML estimates are obtained using a more detailed likelihood of binding and unbinding times introduced in [27], indicating that the signaling scheme studied here might be close to optimal. Despite this similarity, we emphasize that [27] did not address the question of specificity, being focused on the optimality of the concentration sensing.

In a generalization of the one-variable procedure from section II A, the expected estimate uncertainties are given by the typical widths of the posterior/likelihood in the $(c, k_{\rm off})$ space, quantified by the covariance matrix

$$\hat{\boldsymbol{\Sigma}} \equiv \begin{bmatrix}\langle\delta c^2\rangle & \langle\delta k_{\rm off}\delta c\rangle\\ \langle\delta k_{\rm off}\delta c\rangle & \langle\delta k^2_{\rm off}\rangle\end{bmatrix}.$$

Very generally, a lower bound on the covariance matrix of the estimates is given by the inverse of the Fisher Information Matrix (FIM) $\hat{\boldsymbol{\mathcal{I}}}$

$$\hat{\boldsymbol{\mathcal{I}}}(c, k_{\rm off}) \equiv -\begin{bmatrix}\langle\frac{\partial^2 L}{\partial c\partial c}\rangle & \langle\frac{\partial^2 L}{\partial k_{\rm off}\partial c}\rangle\\ \langle\frac{\partial^2 L}{\partial c\partial k_{\rm off}}\rangle & \langle\frac{\partial^2 L}{\partial k_{\rm off}\partial k_{\rm off}}\rangle\end{bmatrix},$$

where L is the logarithm of the likelihood $P(n, m|c, k_{\rm off})$ [72].

In the long time limit, where the likelihood is sharply peaked, the approximate squared relative errors of the estimates are

$$\begin{aligned}\frac{\langle\delta c^2\rangle}{c^2} &= \frac{1}{k_pt}\frac{1+x}{x}\left(x^2+\frac{k_p}{k_{\rm off}}\right)\\ \frac{\langle\delta k^2_{\rm off}\rangle}{k^2_{\rm off}} &= \frac{1}{k_pt}\frac{1+x}{x}\left(1+\frac{k_p}{k_{\rm off}}\right).\end{aligned} \tag{10}$$

The scaled squared relative errors are plotted in Fig. 2. In plain language, the cell is not capable of distinguishing ligands with affinities closer than $\sqrt{\langle\delta k^2_{\rm off}\rangle/N}$. An important consequence of this analysis is that signaling specificity is not determined solely by the differences

between ligand affinities but also depends on the ligand concentrations, and is thus context-dependent. The relative error of the concentration estimate behaves qualitatively similar to that of the non-pleiotropic receptor, diverging in both the low and high x limits. On the other hand, the error in $k_{\rm off}$ inference remains low even in the high-occupancy (high x) regime because the knowledge of both n and m allows accurate determination of the average bound time [27, 53].

The ratio of the concentration sensing error of the pleiotropic receptor (Eq. (10)) to that of the non-pleiotropic receptor (Eq. (5)) is $(x^2 + k_p/k_{\rm off})/((1 + x)^2 + 2k_p/k_{\rm off})$. Since this quantity ranges between $(k_p/k_{\rm off})/(1 + 2k_p/k_{\rm off})$ at low x and 1 at high x, pleiotropy always improves the concentration sensing accuracy. Likewise, the corresponding ratio of the estimator errors for $k_{\rm off}$ is always less than one, indicating that pleiotropy not only enables simultaneous estimation of the concentration and the affinity but generally also increases the specificity of signaling as well. This improvement is non-trivial because our pleiotropic model must estimate two variables, rather than just one variable in the non-pleiotropic case.

C. Discrimination between multiple ligands in a mixture

We now consider the more challenging problem of cross talk in a simultaneous mixture of multiple ligands distinguished by their affinities $k_{\rm off,1}$ and $k_{\rm off,2}$. This problem is common in many signaling contexts such as cytokine and TCR signaling in the immune system, as well as others (e.g. [38, 41, 76–79]). In this section, extending the minimal scheme introduced above, we demonstrate that even in this more challenging case both the identities and concentrations of each ligand can be estimated well based on the pleiotropic receptor outputs.

For simplicity, we confine ourselves here to a mixture of two ligands. Following the approach of the previous section, we assume that the goal of the cell is to infer the affinity $k_{\rm off,\,i}$ and the concentration c_i of each ligand in the mixture. As there are four quantities to infer, we consider an extension of the scheme of Fig. 2(a) whereby four different signaling molecules are produced by the receptor in response to ligand binding. To achieve this we assume that the receptor can be in two different bound states (for each ligand) as seen in Fig. 3(a). Molecularly, these states can be different receptor conformations, different phosphorylation states, or have different binding co-factors present [4].

As in the previous section, we assume that the binding of either ligand immediately induces the release of an m-type molecule m_1 from the receptor; and an n-type sensing molecule n_1 is produced with rate k_p while the receptor remains in this first bound state. Transition to the second state occurs with the rate k_f, and releases a different sensing molecules m_2; accordingly, n_2 molecules are produced (also with rate k_p) while the receptor is in the second state. From either of these bound states, the ligand can unbind with the rate $k_{\rm off,i}$. For simplicity, we follow the common assumption that the transitions from first state to the second are irreversible. Although commonly assumed to be constant, in general k_f may depend on the ligand identity [80], because the energies of both states depend on the ligand binding affinity. We choose the transition rate to be inversely proportional to the affinity $k_f = \alpha/k_{\rm off}$ where α is a constant (see Supplemental Material [71]); this assumption does not affect the main results of the paper, and can be relaxed. Note that although the resulting kinetic scheme resembles the well-known kinetic proofreading (KPR) scheme [25, 81], this is incidental to our results, and it is employed here as a simple model of a multi-state receptor. KPR-type approaches to the cross talk problem will be investigated in more detail elsewhere.

The dynamics of the distribution $P(n_1, m_1, n_2, m_2|c_1, k_{\rm off,1}, c_2, k_{\rm off,2})$ are described by an appropriate master equation, similarly to the previous section (see Supplemental Material [71] for details). For sufficiently long times it is also well approximated by a Normal distribution similar to Eq. (8). The means of n_1, m_1, n_2, and m_2 are given by

$$\begin{aligned}
\langle n_1\rangle &= \frac{k_p t}{1+x_1+x_2}\left(\frac{x_1}{1+\alpha/k_{\rm off,1}^2}+\frac{x_2}{1+\alpha/k_{\rm off,2}^2}\right)\\
\langle m_1\rangle &= k_{\rm on} t\frac{c_1+c_2}{1+x_1+x_2}\\
\langle n_2\rangle &= \frac{k_p t}{1+x_1+x_2}\left(\frac{x_1}{1+k_{\rm off,1}^2/\alpha}+\frac{x_2}{1+k_{\rm off,2}^2/\alpha}\right)\\
\langle m_2\rangle &= \frac{k_{\rm on} t}{1+x_1+x_2}\left(\frac{c_1}{1+k_{\rm off,1}^2/\alpha}+\frac{c_2}{1+k_{\rm off,2}^2/\alpha}\right).
\end{aligned} \tag{11}$$

The explicit expressions for the second moments and the covariances are more complicated, and are presented in the Supplemental Material [71].

Following the same prescription as in the previous section, the estimates of the ligand identities and their concentrations, $c_1, k_{\rm off,1}, c_2, k_{\rm off,2}$ can be obtained based on the measurements of the output variables n_1, m_1, n_2, m_2 using, for instance, a Maximum Likelihood estimator. As before, the lower bounds on the estimate errors are provided by the elements of the Fisher Information Matrix. In this section, we restrict ourselves to a numeric analysis of the FIM due to the added complexity of the resulting expressions compared to the expressions for the single ligand case (see Supplemental Material [71] for details).

The results are shown in Fig. 3. The diagonal elements of $\hat{\boldsymbol{\mathcal{I}}}^{-1}$ shown in Fig. 3(c) provide approximate lower bounds on the mean errors of the estimates of the affinities and the concentrations of both ligands. In addition, Fig. 3(d) shows the determinant of the inverse FIM, $\det(\hat{\boldsymbol{\mathcal{I}}}^{-1})$, which serves as a global measure of the overall estimation error [51, 68]. The blue region in Fig. 3(c) in-

dicates where the error in the estimate is less than 33% of the true value. Accordingly, the blue region in Fig. 3(d) indicates where the overall estimation has low error. As $k_{\text{off},2}$ approaches $k_{\text{off},1}$ the estimation problem becomes ill-posed (i.e. $\hat{\boldsymbol{\mathcal{I}}}$ becomes singular). In this limit, the receptor outputs are no longer independent and so four input variables cannot be estimated simultaneously.

It is instructive to focus on two different regions of the parameter space in Figs. 3(c) and 3(d) which correspond to two well-known sensing problems commonly encountered in a number of cell signaling contexts. One problem, illustrated in the lower part of Fig. 3(b) (orange dashed line), is the specific and accurate sensing of two ligands in a mixture when both have similar affinities and arbitrary concentrations. This type of challenge is commonly present, for example, in cytokine and chemokine signaling in the immune system [41, 59]. This scenario corresponds to the lower regions of the plots in Figs. 3(c) and 3(d), indicated by the orange dashed rectangle (the weaker binding ligand has an affinity that is relatively close to that of the stronger binding ligand). As shown in Fig. 3(c), this is a difficult task to perform, and is possible only in an intermediate range of concentrations where the blue regions in each panel overlap (roughly between $k_{on}c_2/k_p \in [10^{-2}, 10^0]$, or within the 10^4 contour of Fig. 3(d)). This finding might be part of an explanation of the prevalence of dimeric receptors in many signaling pathways, because ligand induced dimerization enhances the differences in the effective binding affinities between similar ligands [22]. Overall, there is a trade-off between the two ligands: a specific estimate of $k_{\text{off},1}$ implies a less specific estimate of $k_{\text{off},2}$; similar trade-off exists for accuracy of the estimation of concentrations c_1 and c_2.

The "T cell antigen" scenario is illustrated in the upper region of Fig. 3(b) (purple dashed line). It represents a different sensing problem, whereby the stronger binding ligand is present at a low concentration on the background of a low affinity ligand present at a high concentration [18, 23, 30]. This scenario corresponds to the upper right region in Figs. 3(c) and 3(d) (indicated by a purple dashed line). The plots of the accuracy and specificity for ligand 1 (two upper panels in Fig. 3(c)) indicate that for sufficiently distinct ligands (i.e. $k_{\text{off},2} \gg k_{\text{off},1}$), sensing of the stronger-binding ligand is not impaired by a wide range of concentrations of the weaker-binding ligand. Interestingly, in this regime overall estimation has low error (blue region of Fig. 3(d)). We discuss the implications of these results in the next section.

III. SUMMARY AND DISCUSSION

Cross talk is common in many signaling pathways, which raises the question of how cells are able to sense and thereby respond appropriately to molecularly similar signals carrying different information through these cross-wired pathways. In this paper, we focused on cross talk at the ligand-receptor level, whereby multiple ligands can act through the same surface receptor. This situation can be encountered in cytokine and chemokine signaling in the immune system [41, 59, 82], developmental pathways [7, 33, 38, 78] and other physiological systems [55, 83]. Ligand-receptor cross talk entails a fundamental problem: it is impossible to discriminate between different cognate ligands based on receptor occupancy alone because the identity of the ligand ("quality") can be confounded by its concentration ("quantity") (e.g. [23, 84]). Equally important, when multiple different ligands can bind to the same receptor, it is unclear how the downstream signaling machinery can distinguish between various combinations of different ligands based on the receptor activity alone.

In this paper, we have investigated one potential solution to this problem - signaling pleiotropy - which commonly accompanies cross talk [41, 46], using models of receptor kinetics that account for the molecular noise at both the receptor and the downstream variables. We mathematically confirmed the intuitive notion that the classical model of a receptor which binds multiple ligands but produces only one type of downstream sensing molecule is not able to simultaneously discern the ligand identity (as defined by its unbinding rate k_{off}), and its quantity as expressed by its concentration c.

In contrast, a pleiotropic receptor, which produces two types of downstream signaling molecules, can resolve this ambiguity. The crucial feature of the model enabling these properties is that the two output signaling molecules reflect physically different features of the ligand-receptor interaction - in the case studied here, one variable is proportional to the bound time of the ligand, while the other reflects the number of distinct ligand-receptor binding events.

Importantly, a realistic feature of our model is that the inference is based only on the numbers of the produced signaling molecules and not on the knowledge of whole sequence of binding-unbinding events that has been a feature of a number of works [27, 52, 53, 85]. In addition to providing a solution to the specificity-accuracy dilemma, our analysis indicates that the noise in the production of the downstream sensing molecules (on top of the receptor binding-unbinding fluctuations) can significantly affect the specificity and the accuracy of molecular sensing compared to the models that only account for the randomness of the receptor-unbinding events [15, 27, 53].

Furthermore, we have shown that with a sufficient number of downstream receptor sensing molecules, a pleiotropic receptor can simultaneously determine the identities and quantify the concentrations of two distinct (and arbitrary) ligands, even when they are present in arbitrary mixtures. Namely, four output variables can be used to determine the four unknown variables - two dissociation constants and two concentrations of the ligands in the mixture. Due to the robust nature of this discrimination scheme, we expect it to generalize to combinations of multiple ligands, whereby a signaling network with $2L$ output molecules can be used to determine the identities

and the concentrations of L ligands in the mixture. One such potential scheme is a KPR-like signaling chain with $2L$ bound states of the receptor. This could provide a foundation for a generic combinatorial signal recognition system in cross-wired pathways. The estimation errors are likely to increase with the number of ligands in the mixture [53], and it remains to be investigated up to what number of ligands the proposed mechanism remains biologically relevant. However, the error can always be lowered by increasing the copy number of receptors or the signaling time. Investigation of how the sensing error scales with the number of ligands is beyond the scope of this manuscript and will be presented elsewhere.

Due to the interplay of molecular and evolutionary constraints, cross talk in receptor signaling systems may be inevitable, and our results indicate that receptor pleiotropy can provide a general mechanism for specific and accurate signaling in such systems. However, signaling cross talk might not be just undesirable "noise" hampering accurate and specific ligand discrimination, but rather might have benefits of its own. For example, the combination of cross talk and pleiotropy may require fewer types of receptors than multiple independent receptors for each ligand, which could lead to lower resource requirements. Additionally, pleiotropic cross-wired signaling networks may be more robust to genetic or structural alterations in the molecular components of the pathway such as the receptors themselves, or the associated the readout molecules and the signaling enzymes.

Our model is constrained by the assumptions about the nature of the output variables n and m, which are inspired by the observed modes of signaling in cytokine and GPCR pathways. It is instructive to compare our results with those based on the inference from the whole sequence of binding-unbinding events (which requires more intricate intracellular molecular networks) [17, 27, 30, 52, 53]. The likelihood of a sequence of binding/unbinding events with overall bound time t_b and the overall number of binding events m is given by $P(t_b, m|c, k_{\rm off}) \sim \exp(-k_{\rm on}ct)\exp(t_b(-k_{\rm off}+k_{\rm on}c))\cdot(k_{\rm off}k_{\rm on}c)^m$ [27]. Maximizing this likelihood over $(c, k_{\rm off})$ results in the same estimates as given by Eq. (9). The corresponding lower bounds on the estimation errors (found by inverting the Fisher Information Matrix) in this case are $\langle\delta c^2\rangle/c^2 = \langle\delta k_{\rm off}^2\rangle/k_{\rm off}^2 = 1/\langle m\rangle$, where $\langle m\rangle = k_{\rm off}tx/(1+x)$. These expressions match Eq. (10) in the limit $k_p/k_{\rm off} \gg 1$ (at finite x); the deviation at finite $k_p/k_{\rm off}$ is a consequence of the additional noise in the production of the signaling molecules on top of the noise of receptor-ligand binding. Thus, our minimal model with only two readout variables appears to be able to take advantage of the full information encoded in the whole sequence of binding-unbinding events. This is likely due to the fact that the Endres-Wingreen likelihood effectively only depends on t_b and m - which are the physical variables "measured" by our variables n and m [17, 27]. This is not true anymore for multiple ligands in a mixture where the likelihood of the time series of the binding-unbinding events retains the explicit dependence on the specific sequence of bound times [17, 30]. In the future, it will be important to investigate what molecular mechanisms might enable cells to access the additional information contained in the sequence of binding-unbinding events [53].

In this paper we have considered only a minimal "module" of a cross-wired receptor signaling network - a receptor of one type capable of interacting with multiple types of ligands. Furthermore, we have assumed that the cell performs estimates of ligand identity and concentration based on the immediate downstream receptor outputs. The ideas of this paper can be extended to the more general case of complex networks of ligands, receptors and downstream signaling molecules that may include positive and negative feedbacks mediated by such molecules [18, 31, 51, 53]. The pleiotropic receptor outputs we considered here may also be used for alternative sensing goals such as detecting changes in the composition of a ligand mixture [17]. Functional pleiotropy can alternatively be achieved by using different stages in the time course of the signaling as distinct output variables [17, 42, 86], facilitated through feedback such as receptor internalization.

Depending on the task that needs to be solved by the cell, different mathematical frameworks might be more appropriate [17]. Among other approaches, the results of this paper also provide an interesting outlook on the information theory approaches to cell signaling [29, 42, 87–90] via connections between the channel capacity of a signaling pathway and the Fisher Information Matrix. Further constraints, such as receptor integration time and energy consumption in the non-equilibrium signaling cycle [24, 67] may be considered in extensions of this work. These lie outside of the scope of the present work, and will be studied in the future. Finally, while this paper has focused on sensing capabilities of single cells, intercellular interactions in multicellular environments can result in collective responses to the signaling milieu leading to collective decisions at the population level [21, 91, 92].

MATERIALS AND METHODS

All calculations and simulations were performed in Python 3.8.3 using NumPy 1.18.5, and Mathematica 10.4. Computational details of the results presented here are provided in the Supplemental Material. The code implementing the analysis, simulations, and plotting is available at `https://github.com/uoftbiophysics/cellsignalling`.

SUPPLEMENTAL MATERIALS

Supplemental Text
section A: Calculating the moments of the output variables

section B: Obtaining Maximum Likelihood Estimates of c and k_{off}
section C: Accuracy of the estimators
section D: Alternative calculation of the moments of the distribution of n and m
section E: Long time distribution well-approximated by a Normal distribution
section F: Bayesian framework, effects of prior
fig. S1. The MLE for x as a function of n
fig. S2. Model 2 MLE as a function of n for fixed m
fig. S3. Comparison of heuristic estimation error and the Cramér-Rao lower bound for Model 2
fig. S4. Long-time distributions of n and m
fig. S5. Estimation with prior
references [93–95]

Acknowledgements. The authors are indebted to numerous colleagues in the field for illuminating discussions. **Funding:** The authors acknowledge the support of the Natural Sciences and Engineering Research Council of Canada (NSERC) through Discovery Grant RGPIN 402591 to A.Z.; CGS-D Graduate Fellowship to M.S. and PGS-D Graduate Fellowship to D.K.
Contributions: D.K., J.R., and M.S. contributed equally to this work. A.Z. devised the project. All authors performed the research and wrote the paper.
Competing interests: The authors declare that they have no competing interests.

[1] E. Laurenti and B. Göttgens, From haematopoietic stem cells to complex differentiation landscapes, Nature **553**, 418 (2018).
[2] S. H. Crossman, S. J. Streichan, and J. P. Vincent, EGFR signaling coordinates patterning with cell survival during Drosophila epidermal development, PLoS biology **16**, e3000027 (2018).
[3] F. Geissmann, M. G. Manz, S. Jung, M. H. Sieweke, M. Merad, and K. Ley, Development of monocytes, macrophages, and dendritic cells, Science **327**, 656 (2010).
[4] H. Lodish, A. Berk, S. L. Zipursky, P. Matsudaira, D. Baltimore, and J. Darnell, *Molecular Cell Biology*, 4th ed. (W.H. Freedman, New York, 2000).
[5] G. Altan-Bonnet and R. N. Germain, Modeling T cell antigen discrimination based on feedback control of digital ERK responses, PLoS Biology **3**, 1925 (2005).
[6] J. Bagnall, C. Boddington, H. England, R. Brignall, P. Downton, Z. Alsoufi, J. Boyd, W. Rowe, A. Bennett, C. Walker, A. Adamson, N. M. Patel, R. O'Cualain, L. Schmidt, D. G. Spiller, D. A. Jackson, W. Müller, M. Muldoon, M. R. White, and P. Paszek, Quantitative analysis of competitive cytokine signaling predicts tissue thresholds for the propagation of macrophage activation, Science Signaling **11**, 1 (2018).
[7] M. Touzot, M. Grandclaudon, A. Cappuccio, T. Satoh, C. Martinez-Cingolani, N. Servant, N. Manel, and V. Soumelis, Combinatorial flexibility of cytokine function during human T helper cell differentiation., Nature communications **5**, 3987 (2014).
[8] W. J. Rappel and H. Levine, Receptor noise and directional sensing in eukaryotic chemotaxis, Physical Review Letters **100**, 228101 (2008).
[9] H. Berg and D. Brown, Chemotaxis in *Escherichia coli* analyzed by three-dimensional tracking, Nature **239**, 500 (1972).
[10] Y. Wang, C.-L. Chen, and M. Iijima, Signaling mechanisms for chemotaxis, Development, growth & differentiation **53**, 495 (2011).
[11] J. Wong-Ng, A. Celani, and M. Vergassola, Exploring the function of bacterial chemotaxis, Current opinion in microbiology **45**, 16 (2018).
[12] G. Micali and R. G. Endres, Bacterial chemotaxis: information processing, thermodynamics, and behavior, Current Opinion in Microbiology **30**, 8 (2016).
[13] H. C. Berg and E. M. Purcell, Physics of chemoreception, Biophysical Journal **20**, 193 (1977).
[14] W. Bialek and S. Setayeshgar, Physical limits to biochemical signaling, PNAS **102**, 10040 (2005).
[15] P. R. ten Wolde, N. B. Becker, T. E. Ouldridge, and A. Mugler, Fundamental Limits to Cellular Sensing, Journal of Statistical Physics **162**, 1395 (2016).
[16] W. Cui and P. Mehta, Identifying feasible operating regimes for early T-cell recognition: The speed, energy, accuracy trade-off in kinetic proofreading and adaptive sorting, PLOS ONE **13**, e0202331 (2018).
[17] E. D. Siggia and M. Vergassola, Decisions on the fly in cellular sensory systems, PNAS **110**, E888 (2013).
[18] P. François, G. Voisinne, E. D. Siggia, G. Altan-Bonnet, and M. Vergassola, Phenotypic model for early T-cell activation displaying sensitivity, specificity, and antagonism., PNAS **110**, E888 (2013).
[19] W. Bialek, *Biophysics: searching for principles* (Princeton University Press, 2012).
[20] J. E. Ladbury and S. T. Arold, Noise in cellular signaling pathways: causes and effects, Trends in biochemical sciences **37**, 173 (2012).
[21] R. Suderman, J. A. Bachman, A. Smith, P. K. Sorger, and E. J. Deeds, Fundamental trade-offs between information flow in single cells and cellular populations, PNAS **114**, 5755 (2017).
[22] S. Fathi, C. R. Nayak, J. J. Feld, and A. G. Zilman, Absolute ligand discrimination by dimeric signaling receptors, Biophys J **111**, 917 (2016).
[23] P. François and G. Altan-Bonnet, The Case for Absolute Ligand Discrimination: Modeling Information Processing and Decision by Immune T Cells, Journal of Statistical Physics **162**, 1130 (2016).
[24] A. H. Lang, C. K. Fisher, T. Mora, and P. Mehta, Thermodynamics of statistical inference by cells, Phys. Rev. Lett. **113**, 148103 (2014).
[25] T. W. McKeithan, G. Voisinne, E. D. Siggia, G. Altan-Bonnet, and M. Vergassola, Kinetic proofreading in T-cell receptor signal transduction., PNAS **92**, 5042 (1995).
[26] L. Song, S. M. Nadkarni, H. U. Bödeker, C. Beta, A. Bae, C. Franck, W. J. Rappel, W. F. Loomis, and E. Bodenschatz, Dictyostelium discoideum chemotaxis: Threshold

for directed motion, European Journal of Cell Biology **85**, 981 (2006).
[27] R. G. Endres and N. S. Wingreen, Maximum Likelihood and the Single Receptor, Physical Review Letters **103**, 158101 (2009).
[28] R. G. Endres and N. S. Wingreen, Accuracy of direct gradient sensing by cell-surface receptors, Progress in Biophysics and Molecular Biology **100**, 33 (2009).
[29] D. Ellison, A. Mugler, M. D. Brennan, S. H. Lee, R. J. Huebner, E. R. Shamir, L. A. Woo, J. Kim, P. Amar, I. Nemenman, A. J. Ewald, and A. Levchenko, Cell-cell communication enhances the capacity of cell ensembles to sense shallow gradients during morphogenesis., PNAS **113**, E679 (2016).
[30] T. Mora, Physical Limit to Concentration Sensing Amid Spurious Ligands, Physical Review Letters **115**, 038102 (2015).
[31] A. Murugan, D. A. Huse, and S. Leibler, Speed, dissipation, and error in kinetic proofreading, PNAS **109**, 12034 (2012), https://www.pnas.org/content/109/30/12034.full.pdf.
[32] K. Banerjee, A. B. Kolomeisky, and O. A. Igoshin, Elucidating interplay of speed and accuracy in biological error correction, PNAS **114**, 5183 (2017).
[33] H. Tran, J. Desponds, C. A. Perez Romero, M. Coppey, C. Fradin, N. Dostatni, and A. M. Walczak, Precision in a rush: Trade-offs between reproducibility and steepness of the hunchback expression pattern, PLOS Computational Biology **14**, e1006513 (2018).
[34] C. Garbers, H. M. Hermanns, F. Schaper, G. Müller-Newen, J. Grötzinger, S. Rose-John, and J. Scheller, Plasticity and cross-talk of interleukin 6-type cytokines., Cytokine & growth factor reviews **23**, 85 (2012).
[35] S. Basak and A. Hoffmann, Crosstalk via the NF-kappaB signaling system., Cytokine & growth factor reviews **19**, 187 (2008).
[36] J. S. Rawlings, K. M. Rosler, and D. A. Harrison, The JAK/STAT signaling pathway., Journal of cell science **117**, 1281 (2004).
[37] C. Thomas, I. Moraga, D. Levin, P. O. Krutzik, Y. Podoplelova, A. Trejo, C. Lee, G. Yarden, S. E. Vleck, J. S. Glenn, P. Nolan, J. Piehler, G. Schreiber, and K. C. Garcia, Structural linkage between ligand discrimination and receptor activation by type I interferons, Cell **146**, 621 (2011).
[38] Y. E. Antebi, J. M. Linton, H. Klumpe, B. Bintu, M. Gong, C. Su, R. McCardell, and M. B. Elowitz, Combinatorial Signal Perception in the BMP Pathway, Cell **170**, 1184 (2017).
[39] D. J. Klinke, N. Cheng, and E. Chambers, Quantifying crosstalk among interferon-γ, interleukin-12, and tumor necrosis factor signaling pathways within a TH1 cell model., Science signaling **5**, 32 (2012).
[40] M. N. McClean, A. Mody, J. R. Broach, and S. Ramanathan, Cross-talk and decision making in MAP kinase pathways., Nature genetics **39**, 409 (2007).
[41] I. Moraga, J. Spangler, J. L. Mendoza, and K. C. Garcia, Multifarious determinants of cytokine receptor signaling specificity., Advances in immunology **121**, 1 (2014).
[42] T. Jetka, K. Nienałtowski, S. Filippi, M. P. Stumpf, and M. Komorowski, An information-theoretic framework for deciphering pleiotropic and noisy biochemical signaling, Nature Communications **9** (2018).
[43] B. N. Kholodenko, J. F. Hancock, and W. Kolch, Signalling ballet in space and time., Nature reviews. Molecular cell biology **11**, 414 (2010).
[44] M. S. Chatterjee, J. E. Purvis, L. F. Brass, and S. L. Diamond, Pairwise agonist scanning predicts cellular signaling responses to combinatorial stimuli, Nature biotechnology **28**, 727 (2010).
[45] G. Schreiber, The molecular basis for differential type i interferon signaling, Journal of Biological Chemistry **292**, 7285 (2017).
[46] K. Ozaki and W. J. Leonard, Cytokine and cytokine receptor pleiotropy and redundancy., The Journal of biological chemistry **277**, 29355 (2002).
[47] J.-X. Lin, T.-S. Migone, M. Tseng, M. Friedmann, J. A. Weatherbee, L. Zhou, A. Yamauchi, E. T. Bloom, J. Mietz, S. John, and W. J. Leonard, The role of shared receptor motifs and common stat proteins in the generation of cytokine pleiotropy and redundancy by IL-2, IL-4, IL-7, IL-13, and IL-15, Immunity **2**, 331 (1995).
[48] J. G. Moggs and G. Orphanides, Estrogen receptors: orchestrators of pleiotropic cellular responses, EMBO reports **2**, 775 (2001).
[49] Y. Tagaya, R. N. Bamford, A. P. DeFilippis, and T. A. Waldmann, Il-15: a pleiotropic cytokine with diverse receptor/signaling pathways whose expression is controlled at multiple levels, Immunity **4**, 329 (1996).
[50] G. Vert and J. Chory, Crosstalk in Cellular Signaling: Background Noise or the Real Thing?, Developmental Cell **21**, 985 (2011).
[51] M. Carballo-Pacheco, J. Desponds, T. Gavrilchenko, A. Mayer, R. Prizak, G. Reddy, I. Nemenman, and T. Mora, Receptor crosstalk improves concentration sensing of multiple ligands, Physical Review E **99**, 022423 (2019).
[52] V. Singh and I. Nemenman, Simple biochemical networks allow accurate sensing of multiple ligands with a single receptor, PLOS Computational Biology **13**, e1005490 (2017).
[53] V. Singh and I. Nemenman, Universal properties of concentration sensing in large ligand-receptor networks, Physical Review Letters **124**, 028101 (2020).
[54] M. Komorowski and D. S. Tawfik, The limited information capacity of cross-reactive sensors drives the evolutionary expansion of signaling, Cell systems **8**, 76 (2019).
[55] A. Zinkle and M. Mohammadi, A threshold model for receptor tyrosine kinase signaling specificity and cell fate determination, F1000Research **7** (2018).
[56] R. Phillips, J. Theriot, J. Kondev, and H. Garcia, *Physical biology of the cell* (Garland Science, 2012).
[57] M. Skoge, Y. Meir, and N. S. Wingreen, Dynamics of cooperativity in chemical sensing among cell-surface receptors, Physical Review Letters **107**, 178101 (2011).
[58] D. Wootten, A. Christopoulos, M. Marti-Solano, M. M. Babu, and P. M. Sexton, Mechanisms of signalling and biased agonism in G protein-coupled receptors, Nature Reviews Molecular Cell Biology **19**, 638 (2018).
[59] C. L. Sokol and A. D. Luster, The chemokine system in innate immunity., Cold Spring Harbor perspectives in biology **7**, a016303 (2015).
[60] K. E. Tkach, J. E. Oyler, and G. Altan-Bonnet, Cracking the nf-κb code, Science signaling **7**, pe5 (2014).
[61] P. Li and M. B. Elowitz, Communication codes in developmental signaling pathways, Development **146**, dev170977 (2019).
[62] P. Nelson, *Physical models of living systems* (Macmillan

Higher Education, 2014).
[63] K. Kaizu, W. de Ronde, J. Paijmans, K. Takahashi, F. Tostevin, and P. R. ten Wolde, The Berg-Purcell limit revisited., Biophysical journal **106**, 976 (2014).
[64] J. Faro, M. Castro, and C. Molina-París, A unifying mathematical framework for experimental TCR-pMHC kinetic constants, Scientific Reports **7**, 46741 (2017).
[65] S. K. Bromley, W. R. Burack, K. G. Johnson, K. Somersalo, T. N. Sims, C. Sumen, M. M. Davis, A. S. Shaw, P. M. Allen, and M. L. Dustin, The immunological synapse, Annual review of immunology **19**, 375 (2001).
[66] D. A. Lauffenburger and J. J. Linderman, *Receptors: models for binding, trafficking, and signaling* (Oxford University Press on Demand, 1996).
[67] C. C. Govern and P. R. Ten Wolde, Optimal resource allocation in cellular sensing systems, PNAS **111**, 17486 (2014).
[68] I. Nemenman and N. Sinitsyn, Time-dependent corrections to effective rate and event statistics in Michaelis–Menten kinetics, IET Systems Biology **4**, 409 (2010).
[69] S. Iyer-Biswas, F. Hayot, and C. Jayaprakash, Stochasticity of gene products from transcriptional pulsing, Physical Review E **79**, 031911 (2009).
[70] M. Pinsky and S. Karlin, *An introduction to stochastic modeling* (Academic press, 2010).
[71] See supplemental material (ancillary files) for technical details.
[72] S. M. Kay, *Fundamentals of Statistical Signal Processing: Estimation Theory* (Prentice-Hall, Inc., Upper Saddle River, NJ, USA, 1993).
[73] J. Piehler, C. Thomas, K. C. Garcia, and G. Schreiber, Structural and dynamic determinants of type I interferon receptor assembly and their functional interpretation, Immunology Review **250**, 317 (2012).
[74] S. R. Neves, P. T. Ram, and R. Iyengar, G protein pathways, Science **296**, 1636 (2002).
[75] A. Mócsai, J. Ruland, and V. L. Tybulewicz, The syk tyrosine kinase: a crucial player in diverse biological functions, Nature Reviews Immunology **10**, 387 (2010).
[76] A. K. Singh, R. K. Arya, A. K. Trivedi, S. Sanyal, R. Baral, O. Dormond, D. M. Briscoe, and D. Datta, Chemokine receptor trio: CXCR3, CXCR4 and CXCR7 crosstalk via CXCL11 and CXCL12, Cytokine & Growth Factor Reviews **24**, 41 (2013).
[77] M. S. Lee and Y.-J. Kim, Signaling pathways downstream of pattern-recognition receptors and their cross talk., Annual review of biochemistry **76**, 447 (2007).
[78] X.-H. Feng and R. Derynck, Specificity and Versatility in TGF-β Signaling Through Smads, Annual Review of Cell and Developmental Biology **21**, 659 (2005).
[79] K. Shuai and B. Liu, Regulation of JAK-STAT signalling in the immune system., Nature reviews. Immunology **3**, 900 (2003).
[80] Y. Savir and T. Tlusty, Conformational proofreading: the impact of conformational changes on the specificity of molecular recognition, PloS one **2** (2007).
[81] D.K. Tischer and O.D. Weiner, Light-based tuning of ligand half-life supports kinetic proofreading model of T cell signaling., eLife **8**, 1–25 (2019).
[82] M. A. Rowland, W. Fontana, and E. J. Deeds, Crosstalk and competition in signaling networks., Biophysical journal **103**, 2389 (2012).
[83] S. Qin, Q. Li, C. Tang, and Y. Tu, Optimal compressed sensing strategies for an array of nonlinear olfactory receptor neurons with and without spontaneous activity, PNAS **116**, 20286 (2019).
[84] P. Francois and A. Zilman, Physical approaches to receptor sensing and ligand discrimination, Current Opinion in Systems Biology (2019).
[85] T. Mora and N. S. Wingreen, Limits of Sensing Temporal Concentration Changes by Single Cells, Physical Review Letters **104**, 248101 (2010).
[86] D. M. Freed, N. J. Bessman, A. Kiyatkin, E. Salazar-Cavazos, P. O. Byrne, J. O. Moore, C. C. Valley, K. M. Ferguson, D. J. Leahy, D. S. Lidke, *et al.*, Egfr ligands differentially stabilize receptor dimers to specify signaling kinetics, Cell **171**, 683 (2017).
[87] G. Tkačik, A. M. Walczak, and W. Bialek, Optimizing information flow in small genetic networks, Physical Review E - Statistical, Nonlinear, and Soft Matter Physics **80**, 031920 (2009).
[88] C. Waltermann and E. Klipp, Information theory based approaches to cellular signaling, Biochimica et Biophysica Acta (BBA)-General Subjects **1810**, 924 (2011).
[89] P. Mehta, S. Goyal, T. Long, B. L. Bassler, and N. S. Wingreen, Information processing and signal integration in bacterial quorum sensing, Molecular systems biology **5**, 325 (2009).
[90] A. C. Barato, D. Hartich, and U. Seifert, Efficiency of cellular information processing, New Journal of Physics **16**, 103024 (2014).
[91] A. Mugler, A. Levchenko, and I. Nemenman, Limits to the precision of gradient sensing with spatial communication and temporal integration., PNAS **113**, E689 (2016).
[92] A. Oyler-Yaniv, J. Oyler-Yaniv, B. M. Whitlock, Z. Liu, R. N. Germain, M. Huse, G. Altan-Bonnet, and O. Krichevsky, A tunable diffusion-consumption mechanism of cytokine propagation enables plasticity in cell-to-cell communication in the immune system, Immunity **46**, 609 (2017).
[93] V. N. Kampen, *Stochastic Processes in Physics and Chemistry* (2007).
[94] J. M. Freeman and R. G. Gallager, Discrete Stochastic Processes., The Journal of the Operational Research Society 10.2307/3009951 (1997).
[95] R. B. Ash and C. A. Doléans-Dade, *Probability & Measure Theory*, 2nd ed. (Academic Press, San Diego, 2000) pp. 307–309.

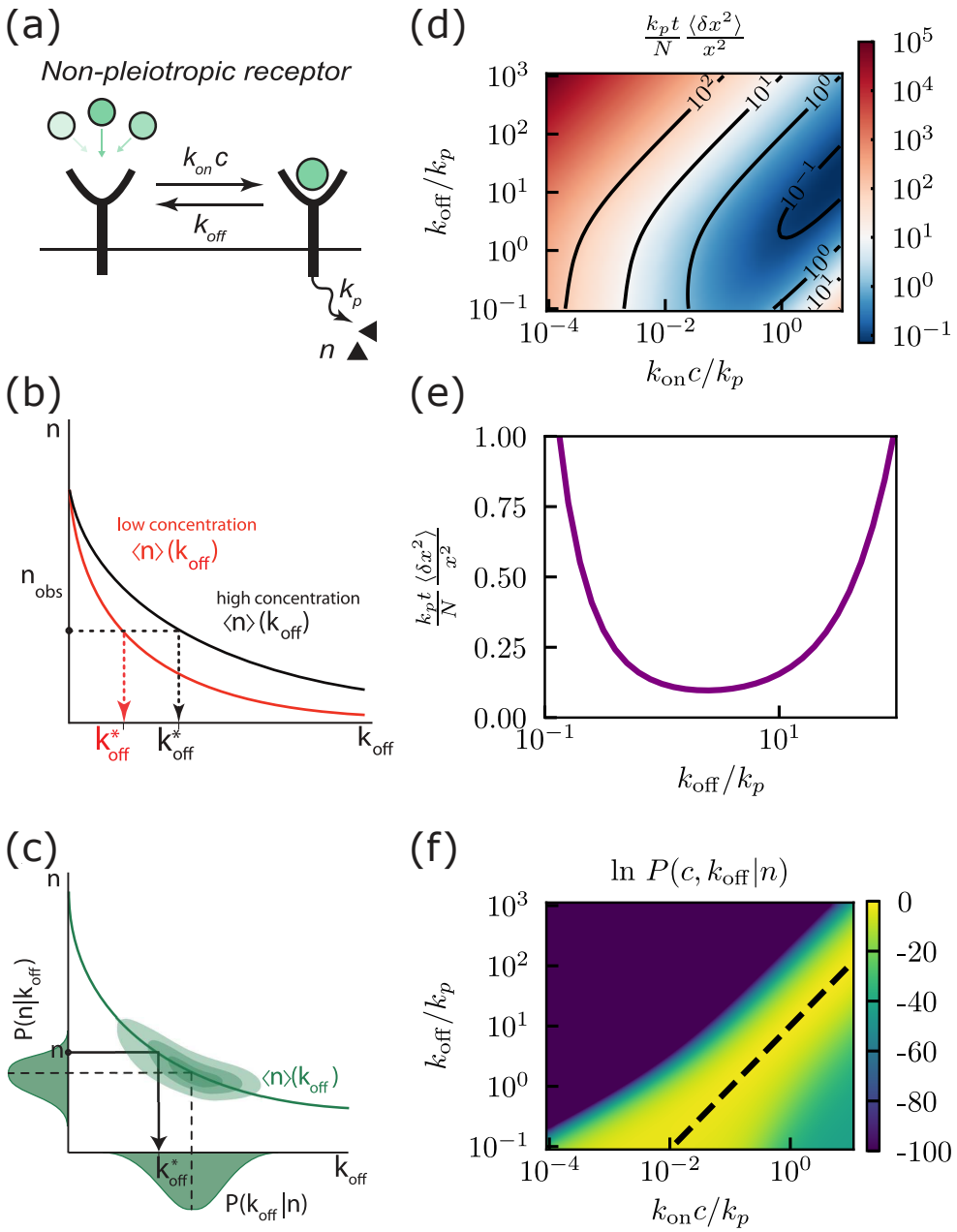


FIG. 1. *Specificity and accuracy for a non-pleiotropic receptor.* (a) Different ligands (shown in different colors) with distinct $k_{\rm off}$ can bind the receptor. When bound by a ligand, the receptor produces downstream signaling molecules n at a rate k_p. (b) An illustration of the fundamental specificity-accuracy problem. The same number of signaling molecules $n_{\rm obs}$ can be produced by a low concentration of a strongly binding ligand as a high concentration of a weakly binding ligand. See text. (c) Fluctuations in n resulting from the stochasticity of the binding-unbinding and production events, described by the probability distribution, $P(n|k_{\rm off})$, lead to an uncertainty in the estimate $k^*_{\rm off}$, encapsulated in the distribution $P(k_{\rm off}|n)$. The width of $P(k_{\rm off}|n)$ is a measure of the uncertainty in the estimate. (d) Squared relative error of the estimate of x as a function of the dimensionless ligand concentration and unbinding rate, scaled by k_pt/N with $k_pt = 10^2$ and $N = 10^2$; see Eq. (5). (e) A cross-section of the heatmap in panel (d), holding $k_{\rm on}c/k_p = 1$. (f) The posterior probability $P(c, k_{\rm off}|n)$ does not have a defined maximum in $(c, k_{\rm off})$ space but instead has a ridge along the line $(\frac{k_{\rm on}c}{k_p}) = (\frac{k_{\rm off}}{k_p})\frac{n}{k_pt}\frac{1}{1-n/k_pt}$; $n = 10^3$ and $k_pt = 10^2$, illustrating the impossibility of simultaneous determination of c and $k_{\rm off}$ by a non-pleiotropic receptor.

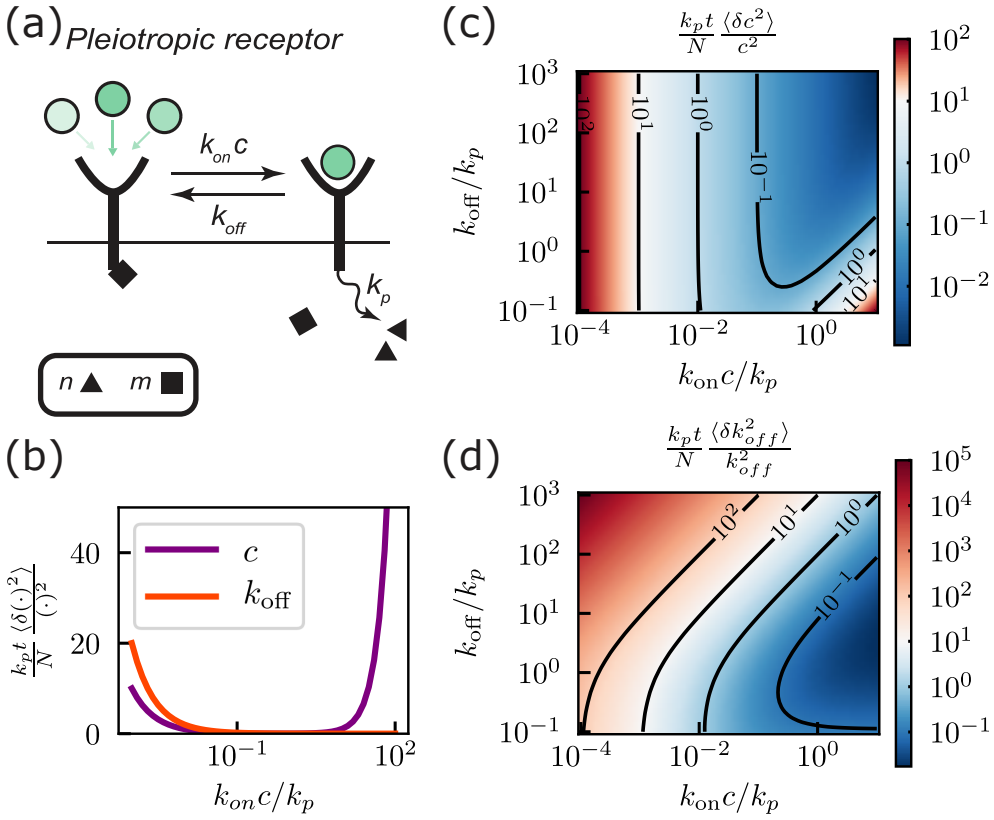


FIG. 2. *Specificity and accuracy of pleiotropic signaling.* (a) The pleiotropic receptor considered here has the same behaviour as in Fig. 1, except that an additional output molecule, denoted as m, is produced for each binding event. (b) The scaled squared relative errors of the estimates for $k_{\rm off}$ (orange) and c (purple) as a function of $k_{\rm on}c/k_p$, holding $k_{\rm off}/k_p = 1$ and $k_p t = 10^2$; see Eq. (10). (c) and (d) Scaled squared relative estimate errors $\frac{k_p t}{N}\frac{\langle\delta k^2_{\rm off}\rangle}{k^2_{\rm off}}$ and $\frac{k_p t}{N}\frac{\langle\delta c^2\rangle}{c^2}$, for $k_p t = 10^2$ and $N = 10^2$.

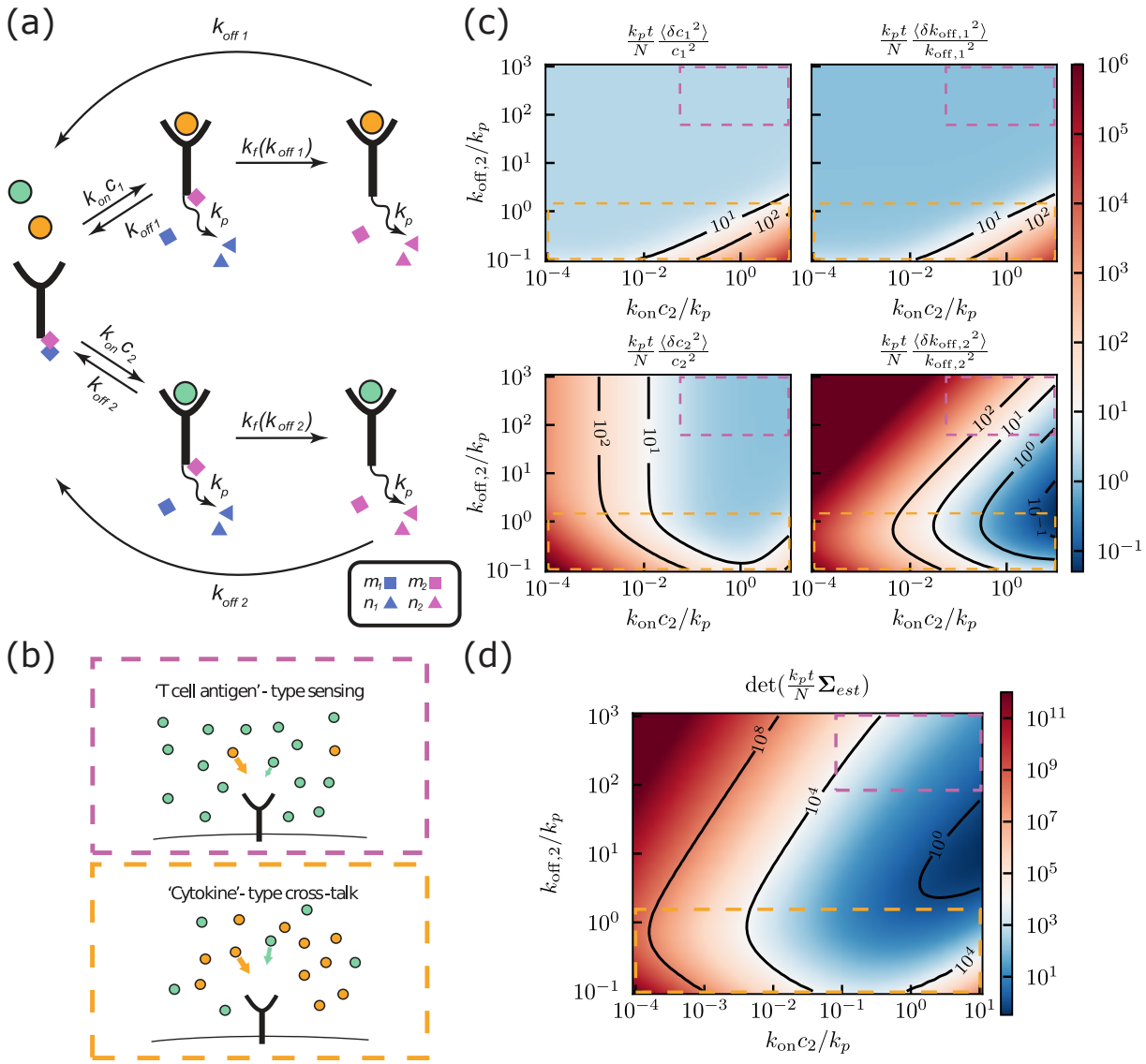


FIG. 3. *Schematic of sensing multiple ligands.* (a) The cross talk receptor considered here produces four distinct sensing molecules when bound. Upon ligand binding, the receptor enters the first bound state from which it releases one m_1 molecule and produces n_1 molecules at rate k_p, analogously to the pleiotropic receptor. Depending on the identity of the bound ligand (encoded through $k_{\rm off}$), the receptor can either unbind or transition to a second bound state with rate $k_f = \alpha/k_{\rm off}$, from which it releases one m_2 molecule and produces n_2 molecules with rate k_p. (b) One cross talk signaling challenge (e.g. cytokines) is to sense two ligands with similar affinities present at arbitrary concentrations. A second cross talk challenge (e.g. T-cell antigens) is to accurately sense a high affinity ligand (large arrow) present at low concentrations while simultaneously sensing a low affinity ligand (small arrow) present at high concentrations. (c) Heatmaps of the diagonal elements of the normalized estimate covariance matrix, scaled by $k_p t/N$. The affinity and concentration of the stronger binding ligand are fixed and the affinity and concentration of the weaker binding ligand are varied. (d) Corresponding heatmap of the determinant of the normalized estimate covariance matrix. The orange (purple) dashed rectangle indicates the region corresponding to the 'cytokine' ('T-cell antigen') type challenge illustrated in (b). Parameters used are $\alpha/{k_p}^2 = 0.2$, $k_p t = 10^2$, $N = 10^2$, $k_{\rm on} c_1/k_p = 10^{-1}$ and $k_{{\rm off},1}/k_p = 10^{-2}$.